RAPID COMMUNICATIONS

PHYSICAL REVIEW B VOLUME 47, NUMBER 11 15 MARCH 1993-I

Photoelectron forward-scattering attenuation from the Cu(001) surface

L. J. Terminello
Lawrence Livermore National Laboratory, Livermore, California 94550

J. J. Barton
IBM Thomas J. Watson Research Center, P.O. Box 218, Yorktown Heights, New York 10598

(Received 9 December 1992)

Photoelectron angular distribution patterns from a single-crystal Cu(001) surface have produced dips, or "silhouettes," in the low-energy, electron angular distribution measured around normal emission—a forward-scattering geometry that at higher energy produces a peak, or enhancement, in electron intensity. We have measured isoenergetic $l=1$ and $l=2,0$ photoelectrons that give different angular distribution patterns. These differences, and the low-energy electron intensity attenuation, are consistent with an electron scattering model that relies on the orbital angular momentum final-state dependence of the diffracting electron.

Beginning with the prediction that localized electron emission from ordered samples underwent geometry-dependent diffraction,[1] electron angular distribution patterns (ADP's) measured from solid-state samples have been used as an atomic-resolution structural probe. Experimental photoelectron and Auger electron diffraction provide the most precise and accurate structural information when they are compared[2,3] to quantum scattering models of the electron emission. However, these electron scattering models came into question when isoenergetic Auger electrons and photoelectrons from single-crystal Cu produced different ADP's (Ref. 4)—a surpising result since a simple scattering model would have predicted the two patterns to be similar. In that work, low-energy photoelectron ADP's revealed a peak in the emission intensity where there was a known forward-scattering condition, yet an Auger electron ADP at the same energy revealed a dip in the electron intensity.

After this experimental result was observed, theoretical reports[5–7] attributed the difference between Auger electron and photoelectron ADP's to differences in the orbital angular momentum (l) of the emitted electron wave. It was asserted that higher l emitted waves, like the predominantly $l=3$ Cu $M_{2,3}M_{4,5}M_{4,5}$ Auger electron, experienced a greater centrifugal barrier on the emitting atom, leading to a phase lag of this wave compared to a lower l electron wave at the same energy. This additional phase pushes the otherwise constructive interference condition—leading to a peak in the forward electron scattering direction—into a destructive-interference condition—an intensity dip. This interpretation extends earlier quantum scattering models of electron diffraction[8] by including the effect of the source wave angular momentum. It demonstrates that the ballistic-electron propagation models, which were created to explain Auger electron scattering silhouettes, are not necessary.[9] The quantum scattering model of electron forward scattering predicts silhouettes in the Auger electron ADP at low energy, high l, and short interatomic scattering distances.

At the same time, Klebanoff and Van Campen[10] observed differences in photoelectron forward-scattering intensities measured at different energies and attributed these intensity changes to the electron angular momentum final state. The Auger electron and photoelectron source-wave dependence suggests that *any* emitted localized electron, regardless of its orbital angular momentum l, should produce a dip in the electron ADP at some energy. Here we report photoelectron forward-scattering silhouettes that confirm the solid-state electron propagation model of Barton and Terminello[5] and others.[6,7]

Photoemission selection rules ($\Delta l=\pm 1$) place greater limitations on possible l emission channels than the Auger emission process. Performing the photoemission experiments with synchrotron radiation allows tuning the electron kinetic energy to identify the energy dependence of the silhouetting and enables an isoenergetic comparison between $l=1$ (Cu $3s$) and $l=0,2$ (Cu $3p$) photoemission ADP's. Together, photoemission selection rules and variable electron energy give a more direct and unambiguous evaluation of our understanding of electron scattering at low energies. Our experiment identifies the angular-momentum-dependent, low-energy bound for using forward-scattering peaks in electron ADP's as a solid-state structural tool.

We measured electron angular distributions from a clean[11] Cu(001) sample using a display-type, electron energy analyzer.[12] This device preserves the angular trajectories of electrons emitted from a solid sample while simultaneously it serves as an energy filter. The fixed-energy, angle-dependent electron distributions were digitized and stored for later evaluation. We measured the Cu $M_{2,3}M_{4,5}M_{4,5}$ Auger electron and Cu $3s$ and $3p$ photoelectron ADP's at low kinetic energy using the monochromatic synchrotron radiation produced at BL-U8 at the National Synchrotron Light Source.[13] This $6M$ toroidal grating monochromator selected the photons required to eject Cu $3s$ (binding energy, 122 eV) and Cu $3p$ (binding energy, 75, 77 eV) electrons at low kinetic energies.

For each ADP an isoenergetic background (i.e., without any spectroscopic features), was collected by

moving the photon energy to place the photopeak outside the analyzer energy window. These background electron intensity patterns divided the photopeak ADP's as an analyzer-throughput and a photon-flux normalization. Once normalized to the empirical background, the patterns displayed a clear fourfold symmetric electron intensity distribution that was partly affected by a prediffraction, atomiclike photoemission final-state amplitude. These are electron intensity anisotropies not related to structure but are caused by photoemission selection rules and are manifested as an angle-dependent intensity that is present before diffraction takes place. To eliminate the final-state photoemission effects, improve the signal to noise ratio, and isolate the electron diffraction inherent in the ADP's, we symmetry averaged the data. Many different forward-scattering trajectories within the near-surface region of our Cu(001) sample could lead to intriguing peak or dip patterns depending on the interatomic distance. We have chosen to display only an emission cone of 57° centered about the surface normal, even though an angular pattern of 84° acceptance was measured. By measuring near-normal emission ADP's we minimized the effects of refraction on the interpretation and isolated one near-surface forward-scattering direction. The Cu $3s$ and $3p$ electron ADP's that we measured at several energies are shown in Fig. 1 compared with the Cu $M_{2,3}M_{4,5}M_{4,5}$ Auger electron ADP. For each image, the full range of electron intensity was scaled to the gray scale shown.

The Cu $M_{2,3}M_{4,5}M_{4,5}$ Auger electron ADP and the 44-eV Cu $3p$ photopeak display the same structure in this measurement as was observed in our earlier report.[4] The $3p$ photopeak that was coincident with the Cu Auger electron emission (isoenergetic) displayed a strong forward peak as does the 44-eV pattern shown; we have displayed the 44-eV peak to better isolate the kinetic energy at which a dip in the normal-emission electron ADP appears. Directly below the two images are the Cu $3s$ and $3p$ photoelectron angular distributions that were measured at lower energies.

The Cu $3s$ photoemission has the simplest angular momentum final state ($l=1$ only) of the three we have measured (Cu $3p$, $l=0,2$; and Cu $M_{2,3,}M_{4,5}M_{4,5}$, predominantly $l=3$). From Fig. 1 it is apparent that the normal emission peak in electron intensity persists down to 24 eV for the Cu $3s$. Throughout this series the intensity of the forward peak diminishes, and between 24 and 19 eV the constructive interference condition becomes destructive thereby leading to a dip in the normal emission ADP at an energy lower than that observed for a predominantly $l=3$ Auger electron. Even at a kinetic energy of 14 eV (not shown) the Cu $3s$ electron ADP still shows a dip. This correlates well with the prediction offered by Barton and Terminello[5] that for some fixed near-surface scattering geometry any l emitted electron will show a dip at a low enough kinetic energy. We have identified this condition for the $l=1$ wave at normal emission ($R=3.51$ Å) from Cu(001).

The Cu $3p$ emission case is more complex to interpret because the final state for $3p$ emission is a combination of $l=0$ and 2.[14] Goldberg, Fadley, and Kono[15] have published a compilation of energy-dependent radial matrix element calculations for Cu and several other elements. This helpful tabulation of branching ratios and cross sections lists that at 40 eV above threshold, the Cu $3p$ initial state populates both channels of the $l=0$ and 2 final states, but a clear preference for the $l=2$ state is indicated.

The electron ADP for Cu $3p$ at 44 eV displays a peak in the normal emission direction thus indicating that constructive interference still dominates—even for the mixed $l=0$ and 2 diffraction wave. However, a dip has begun to form at 39 eV in this forward-scattering direction. Qualitatively, the energy at which this mixed l wave (even though dominated by the $l=2$ wave) starts to de-

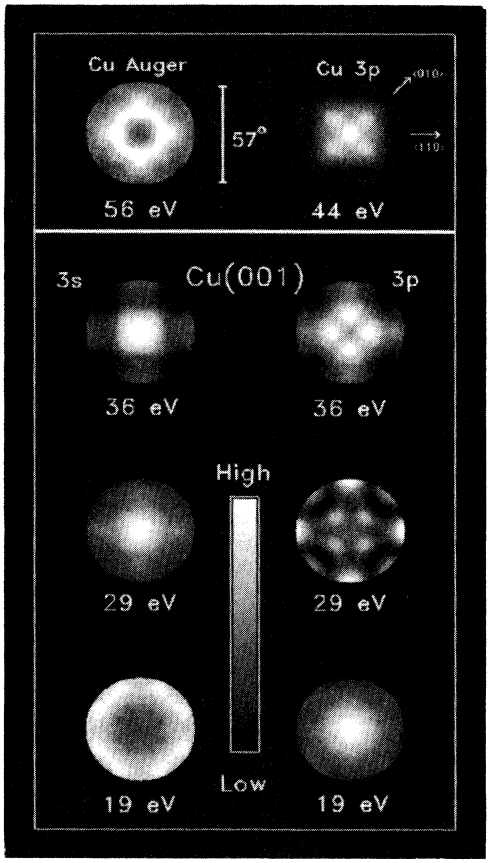

FIG. 1. The angular distribution patterns for Cu $3s$ and $3p$ photoelectrons and $M_{2,3}M_{4,5}M_{4,5}$ Auger electrons measured from the Cu(001) surface. Each image has normal emission in the center and is 57° wide. The top panel shows the $M_{2,3}M_{4,5}M_{4,5}$ Auger electron ADP measured at 56 eV compared to a 44-eV Cu $3p$ photoelectron angular distribution. The two columns of images below the top panel are (on the left) the Cu $3s$ and (on the right) the Cu $3p$ photoelectron ADP's measured at 36, 29, and 19 eV (from top to bottom). The onset of putative electron scattering that leads to a normal emission dip in the electron intensity varies according to the scattering electrons angular momentum ($l=1$ for the $3s$, and a mixture of 0 and 2 for the $3p$). The lower the l, the lower the energy at which the dip appears.

structively interfere is between 44 and 39 eV, and between 39 and 29 eV, the dip in normal emission varies little. We can attribute the small changes in our $3p$ measurements between 39 and 24 eV to the gradual shift in the orbital angular momentum population ratio from mainly $l=2$ to $l=0$.[15] As the Cu $3p$ emission increasingly populates the $l=0$ channel with lowering energy, the total emitted wave experiences a phase-change owing to the interference between the $l=2$ and 0 channels,[14] thus countering the putative effects of lowering energy. Therefore, at 19 eV we see a peak reappear in the Cu $3p$ normal emission, where at slightly higher energy these were the beginnings of a dip in the electron intensity. The Cu $3p$ photoelectron wave at 19 eV still has not reached the destructive interference condition that the isoenergetic Cu $3s$, $l=1$ wave attained. While, the branching ratio changes described in the work of Goldberg, Fadley, and Kono[15] support our observations, further detailed theoretical calculations of the ADP's will be needed for a more quantitative interpretation.

Several points are apparent from these measurements: first, there is a clear difference in the low-energy electron ADP measured at the same kinetic energy for different l waves. The photoemission final-state selection rules are restrictive enough to ensure that different final-state angular momentum photoelectron ADP's can be compared directly in this isoenergetic study. This phenomenon was predicted recently,[5] but this is the first isoenergetic measurement that allows us to state there is a clear difference in electron ADP intensities for differing angular-momentum photoemission source waves.

Second, we have observed that at low enough kinetic energies, a photoelectron forward-scattering condition in an ordered lattice gives rise to a silhouette in the electron ADP. These scattering conditions would otherwise give a peak in intensity, and do so for localized electron emission at higher kinetic energies. The onset of silhouetting—destructive interference— can be determined by the l, R, k (electron energy), and Z (atomic number) of the scattering system.[5] In general the smaller the k and R, and the larger the l, the more likely a destructive interference condition occurs thereby resulting in a dip, or silhouette, in the electron ADP. Determining the exact energy at which the onset occurs is obfuscated by the uncertainty in the inner potential; the electron scattering energy within the crystal is actually higher than we can measure outside the sample by 10–15 eV.[16] Nonetheless, our experimental observation of a forward scattering dip in the electron ADP for $3s$ Cu (001) photoemission gives us a useful lower bound for predicting the occurrence of destructive photoelectron forward scattering.

Electron backscattering as a possible cause of electron intensity attenuation must also be considered, especially because at kinetic energies below 100 eV, electron backscattering can be up to 40–50 % of forward-scattering intensities.[8] Nominally, if backscattering were the cause of the dips in our low kinetic energy ADP's, then it should be present in both the $3s$ and $3p$ ADP's at the same kinetic energy. An intensity attenuation owing to an l-dependent backscattering contribution is invalid here,[14] because the electron scattering factors are computed from a manifold of partial waves and are identical for different l emission waves at the same kinetic energy.[4–7] However, if there is a quantitative difference in phase ($\approx\pi$) for different l waves, then an otherwise constructive backscattering condition could become a destructive one. This is the same reason why a forward-scattering peak turns into a dip for higher l isoenergetic scattering waves. Thus, the origin of the electron intensity attenuation must originate at the emission point and can be attributed to the source wave orbital angular momentum. In fact, our observations are well described by quantum scattering calculations that include multiple scattering and take into account all aspects of electron scattering.[8] However, more detailed theoretical work is needed to quantify the contribution of forward scattering or backscattering on the low-kinetic-energy, normal-emission photoemission intensity.

The issue of multiple chain scattering that leads to defocusing at higher kinetic energies can be neglected in our experiment. Again, if there were some scattering process at the root of the electron attenuation, it should have been observable in both the Cu $3s$ and $3p$ ADP's at the same energy. With regard to multiple-scattering contributions to the electron attenuation, the effect of destructive interference that we see has been predicted to be due to a single-scattering process.[5] Also, it is unlikely that multiple chain scattering could be responsible for our observations because of the limited electron mean free path at our kinetic energies.

Our results clarify some of the recent misinterpretations of electron ADP's, particularly those of low-energy Auger electrons.[9] Using the well-defined orbital angular momentum of the photoemission final state, we have isolated an instance where an $l=1$ photoelectron gave a silhouette in a forward-scattering condition that at higher energies consistently gave a peak. Quantitative statements for the Cu $3p$ electrons will need more study because of the $l=2$ and 0 wave mixing, but our observations are consistent with l-dependent scattering model predictions. Only with accurate and precise methods of modeling electron ADP's from solid systems can improved atomic structural information be obtained.

We would like to thank C. Costas and J. Yurkas for technical assistance with the experiment. This work was conducted under the auspices of the U.S. Department of Energy by the Lawrence Livermore National Laboratory under Contract No. W-7405-ENG-48, and was performed at the National Synchrotron Light Source, Brookhaven National Laboratory, which is supported by the Department of Energy (Division of Materials Sciences and Division of Chemical Sciences of Basic Energy Sciences) under Contract No. DE-AC02-76CH0016.

[1]A. Liebsch, Phys. Rev. Lett. **32**, 1203 (1974).
[2]C. S. Fadley, *Synchrotron Radiation Research: Advances in Surface Science* (Plenum, New York, 1990).
[3]W. F. Egelhoff, Jr., Surf. Sci., **141**, L324 (1984).
[4]L. J. Terminello and J. J. Barton, Science **251**, 1281 (1991).
[5]J. J. Barton and L. J. Terminello, Phys. Rev. B **46**, 13 548 (1992).
[6]D. K. Saldin, G. R. Harp, and B. P. Tonner, Phys. Rev. B **45**, 9629 (1992).
[7]T. Greber, J. Osterwalder, D. Naumović, A. Stuck, S. Hüfner, and L. Schlapbach, Phys. Rev. Lett. **69**, 1947 (1992); Y. U. Idzerda and D. E. Ramaker, *ibid.* **69**, 1943 (1992).
[8]J. J. Barton, S. W. Robey, and D. A. Shirley, Phys. Rev. B **34**, 3807 (1986).
[9]D. G. Frank, N. Batina, T. Golden, F. Lu, and A. T. Hubbard, Science **247**, 182 (1990).
[10]L. E. Klebanoff and D. G. Van Campen, Phys. Rev. Lett. **69**, 196 (1992).
[11]C. C. Bahr, J. J. Barton, Z. Hussain, S. W. Robey, J. G. Tobin, and D. A. Shirley, Phys. Rev. B **35**, 3773 (1987).
[12]D. E. Eastman, J. J. Donelon, N. C. Hien, and F. J. Himpsel, Nucl. Instrum. Methods **172**, 327 (1980).
[13]F. J. Himpsel, Y. Jugnet, D. E. Eastman, J. J. Donelon, D. Grimm, G. Landgren, A. Marx, J. F. Morar, C. Oden, R. A. Pollack, J. Schneir, and C. Crider, Nucl. Instrum. Methods Phys. Res. **222**, 107 (1984).
[14]D. J. Friedman and C. S. Fadley, J. Electron Spectrosc. Relat. Phenom. **51**, 689 (1990); D. E. Parry, *ibid.* **49**, 23 (1989).
[15]S. M. Goldberg, C. S. Fadley, and S. Kono, J. Electron Spectrosc. Relat. Phenom. **21**, 285 (1981).
[16]J. B. Pendry, *Low-Energy Electron Diffraction* (Academic, London, 1974).

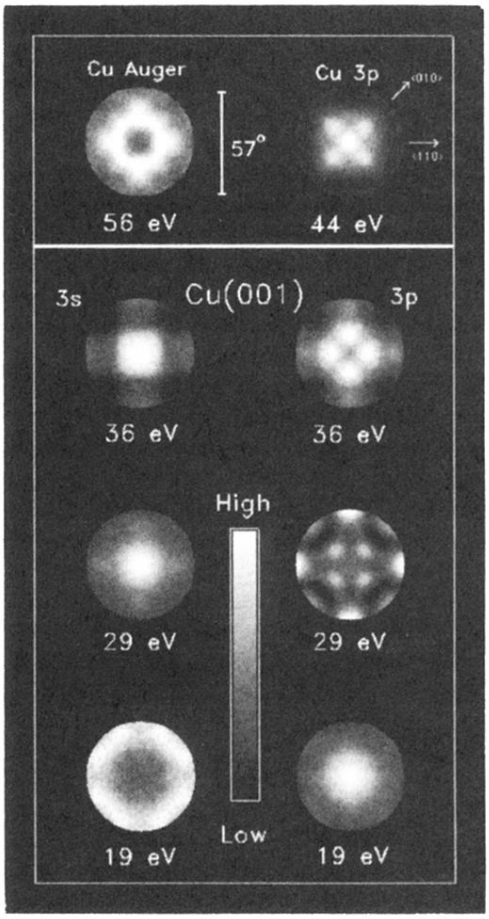

FIG. 1. The angular distribution patterns for Cu 3*s* and 3*p* photoelectrons and $M_{2,3}M_{4,5}M_{4,5}$ Auger electrons measured from the Cu(001) surface. Each image has normal emission in the center and is 57° wide. The top panel shows the $M_{2,3}M_{4,5}M_{4,5}$ Auger electron ADP measured at 56 eV compared to a 44-eV Cu 3*p* photoelectron angular distribution. The two columns of images below the top panel are (on the left) the Cu 3*s* and (on the right) the Cu 3*p* photoelectron ADP's measured at 36, 29, and 19 eV (from top to bottom). The onset of putative electron scattering that leads to a normal emission dip in the electron intensity varies according to the scattering electrons angular momentum ($l=1$ for the 3*s*, and a mixture of 0 and 2 for the 3*p*). The lower the l, the lower the energy at which the dip appears.